Enhancing a LArTPC with a magnetic field

Lorenzo Unich[1]

[1] *Università degli Studi di Napoli "Federico II", Dipartimento di Fisica "Ettore Pancini", Naples, 80126 Italy*
[1] *unichlorenzo@gmail.com*

CONTENTS

1. INTRODUCTION

This paper presents the results of the 2024 Summer Students Italian program at the Fermi National Accelerator Laboratory completed by participant Lorenzo Unich, which lasted between the 27^{th} of July and the 29^{th} of September. This project, which bears the same title of this paper, was supervised by Marco del Tutto, researcher at the Fermi National Accelerator Laboratory. In the first section, we introduce the instruments used throughout the project, detailing their origins and the goals of the traineeship. The second section presents the hardware work conducted, while the final section focuses on the simulations performed for the experimental apparatus. Unless otherwise cited, all pictures and graphs are original.

A. Liquid Argon Time Projection Chambers (LArTPC) ([4], [6])

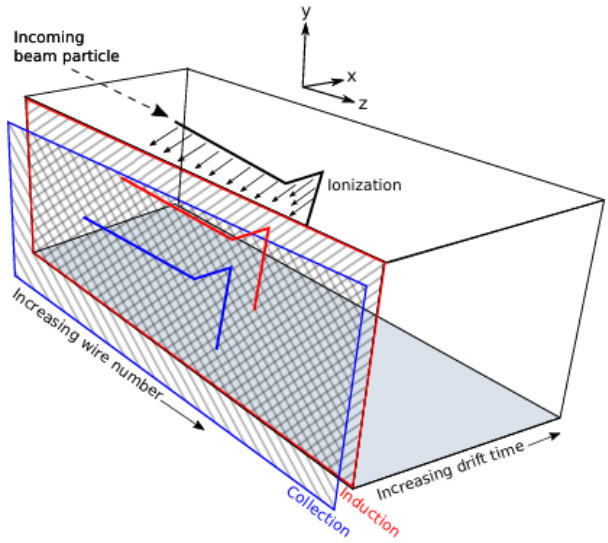

Fig. 1. A general simple scheme for a Time Projection Chamber ([1])

A Time Projection Chamber is a cutting edge detector in particle physics. In a nutshell, it is a device that works thanks to the ionization of liquid argon by the particles that are aimed to be detected; this creates a ion electron pairs; the electrons then drift toward the **sensing planes**, thanks to an electric field. Without a field, in fact, the electrons of the trail produced by a ionising particle would recombine with the ion, shortly after the pair is created. This plane is made up by conducting wires, which detect the charge, eventually read out by an appropriate electronics. The orientation of the wires in each plane is different, providing multiple 2D projections of the same particle event. By combining these 2D projections, the full 3D trajectory of a particle can be reconstructed. Liquid Argon TPCs have been developed after gaseous TPCs; the latter have been used in numerous collision experiments, such as PEP-4 at SLAC or NA49 at CERN. The disadvantage of using TPC with gases is that the density of gaseous materials is much lower than the ones of a liquid: as a consequence, the deposited energy by particles (and hence the energy released by the medium both by ionization and scintillation) are much lower. It is nonetheless interesting using a noble gas for this purpose: the ionization energy of these is higher, hence reducing the possibility of ionization by thermal electrons. Another important parameter to consider for the gas to use, is having a considerable Z, since $X_0 \propto \frac{A}{Z^2}$. Alongside with the fact that it is relatively cheap to produce (since it is present in the atmosphere), these are the reasons of the usage of argon in TPCs. Making it liquid has some advantages: first of all, reducing thermal noise, both in electronics, then in the detector itself; moreover, it increases the density by three orders of magnitude, hence considerably increasing the probability of interaction between particle and Argon. The drawback is that the temperature to make this happen (using a the atmospheric pressure) is 87 K: this requires a cryogenic system to keep the temperature of Argon low and an appropriate electronic which works well at those temperatures.

A.1. Advantages of using a LArTPC in a magnetic field

As previously said, LArTPC are state-of-the-art detectors; nonetheless there is a in gaseous TPC also a magnetic field was added.

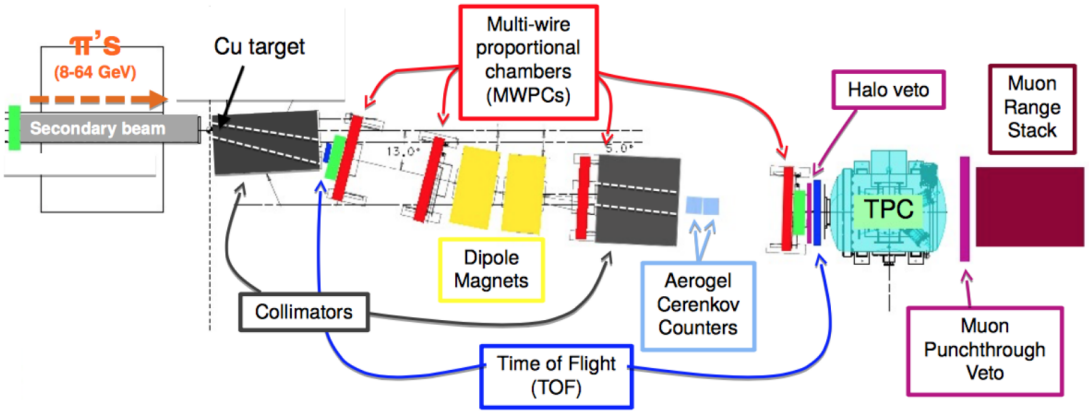

Fig. 2. The setup of LArIAT experiment [1]

Fig. 3. The Jolly Gigant Green (JGG) magnet

This would be a very important component, since it gives mainly three advantages:

- Discriminating the charge sign of the ionising particle
- More ease in reconstructing particle momentum
- Help distinguishing between electronic and photonic showers

It is important to say that charge separation is very important in order to distinguish neutrino and anti neutrino interactions, hence measuring the cross sections of their processes independently. Increasing the momentum measurement's precision and being able to distinguish between photonic and electronic showers are both very desirable effect that derive from the usage of a sufficient magnetic field. If the research yields to positive results, this detector could be used in the context of future neutrino experiments, like DUNE.

B. LArIAT ([1])

This was an R & D project which mainly had two aims: reducing noises and uncertainties in neutrino detection, by experimenting a LArTPC and do precise for cross sections of particles with Argon. Located in the Fermilab Test Beam Facility (FTBF), it characterized one of Fermilab's LArTPC, both in Short-Baseline and in Long-Baseline.

The setup is presented in figure 2: a beam of pions is sent on a Cu target. The experiment then selects the resulting particles just from a particular angle (about 13°). After the interaction with the target, there is a various number of particle that is produced, which is shown in figure The beamline's path is also visible in figure 2.

C. The ArCS project ([2])

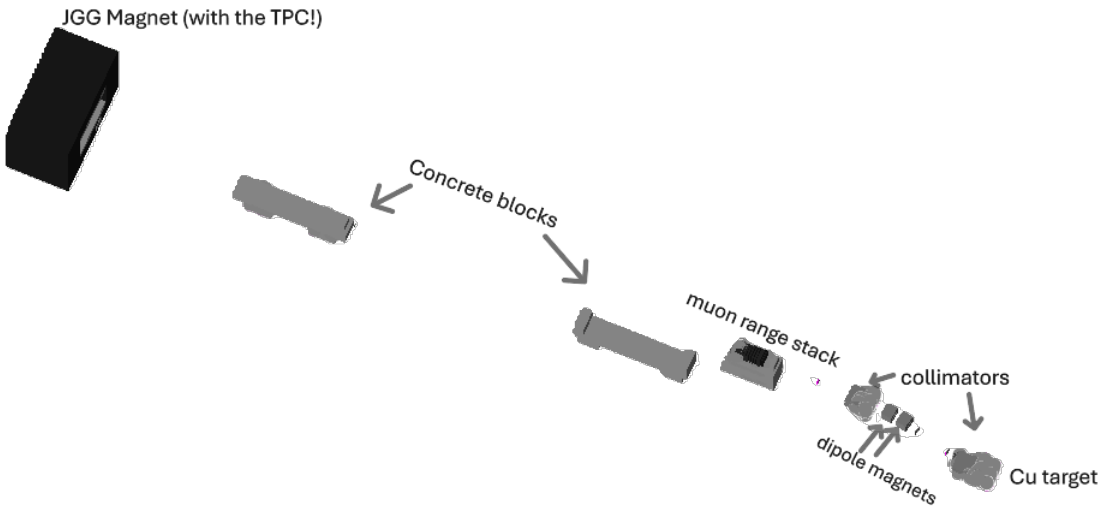

Fig. 4. ArCS experiment's setting, represented in G4Beamline.

It is a research and development experiment, that wants to understand how feasible it is to use a magnetised LArTPC (the advantages of this have already been explained in section A.1). This experiment re-uses the LArIAT's TPC, beamline and electronics, but the extact setting is the one shown in figure 4; the related electronics is sketched in figure 5. A custom cryostat has been built for ArCS, that hosts the LArIAT TPC and will be placed inside the Jolly Green Giant (JGG) magnet at the Fermilab Test Beam Facility. The magnet is shown in Figure 3. The JGG can provide a field which is at most $|\vec{B}^{max}| = 0.7T$. Still, our goal is using the minimum field possible that guarantees reasonably evident curvature and charge separation, both for engineering and cost reasons. The initial part (up to muon range stack) is the same used by LArIAT, while the rest is new.

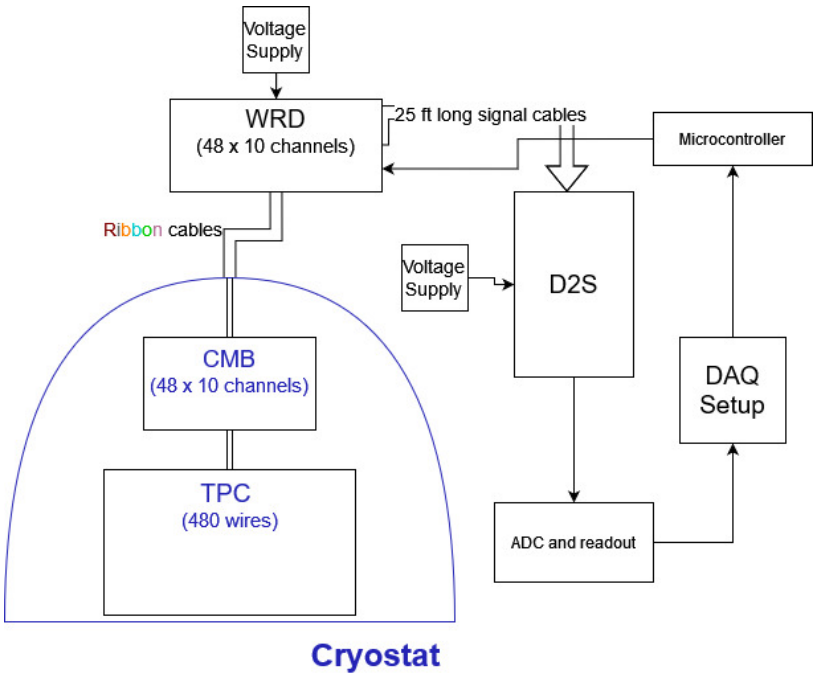

Fig. 5. The electronics configuration that will be used during the ArCS experiment

D. The goal of the internship, in a nutshell

During the internship at Fermilab national laboratory, the goal was working both on hardware and software tasks. These two

kinds of tasks were performed throughout the working period. Here we will briefly introduce them, but they will be expanded in sections 2 and 3, respectively.

Hardware First of all we had to test all the boards that were used in the LArIAT experiment. Secondly, we had to test a configuration that was closer to the one that will be used in ArCS. In order to do this, we had to solder some boards to adapt the cables coming from the *cold boards* and use them with the flanges. The continuity test for the adapting boards was also done in cold nitrogen.

Software The software task was mainly to simulate the beamline on our new experimental apparatus. The Simulation was performed trough the software G4beamline, which is a particle detector simulation program based on Geant4, optimised for beamlines. The goal of this part was understanding how varying the magnetic field affects the flux of particles of an hypothetical electron beamline, passing trough the experimental setup.

2. HARDWARE AND TESTING WORK

A. Testing the LArIAT boards

([1], [5]) The first task was thus testing the electronics that was used in LArIAT. The setting that was used for this phase is represented in fig 6. The core part of the setting are the three kind of printed circuit boards: **Cold Mother Boards** (CMBs), **Warm Receiver Drivers** (WRDs) and **Differential to Single ended** (D2Ss).

A.1. Setting for the tests

CMBs are the only ones that have to be in the cryostat, hence are the only ones that have to be tested for cryogenic temperatures. Their goal is essentially receiving the signals generated by the TPC and transmitting them correctly to the WRDs. There is a total of 10 boards, each one of these had 48 input channels. Each of these boards, includes three ASICs, each one of which has 16 channels. A ribbon cable has the role to connect the CMB to the WRD.
There are 10 WRDs boards, with 48 channels. They process the signals that arrive from the CMBs and can, in case it is required, send new firmwares to the CMBs. They can also send testing signals to the CMBs.
D2S boards take as an input a differential signal (coming from the WRDs) and transforms it in a single ended signal. There are 8 D2Ss boards, since the WRDs have 3×16 exit pins (one exit for each ASIC), whilst D2Ss boards have 4×16 inputs.
In order to test the boards, the setting represented in fig 6 has been adopted.

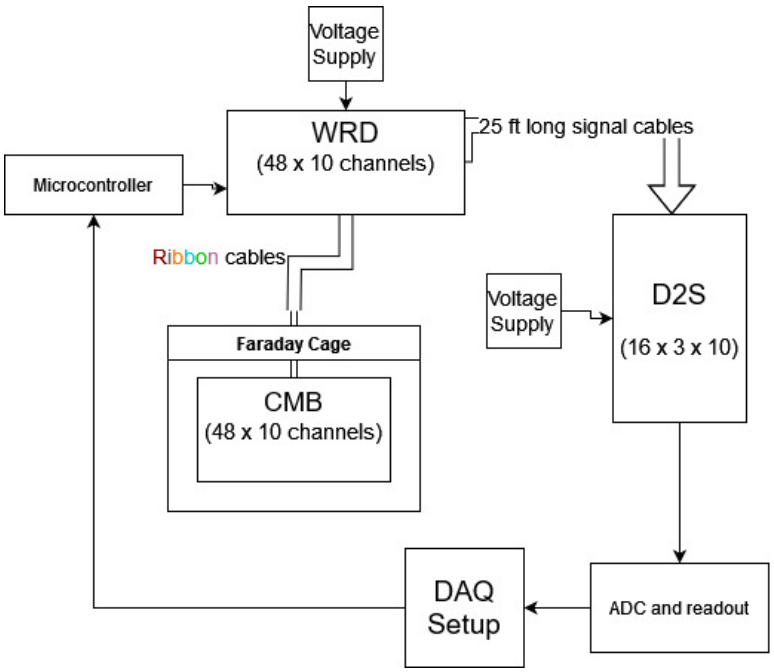

Fig. 6. The setting used to test the CMBs, WRDs and D2Ss.

The cold boards have been placed in a Faraday Cage, in order to reduce the noise [1]. Both the WRDs and the D2Ss are housed in a crate. The CMBs and the WRDs are linked with a Mini D Ribbon Cable. Another ribbon cable ties the D2S crate with a board with some testing pins; each pin represents a channel of the WRD (and hence, if the connection is correct, a CMB channel). The sole purpose of this pin board is making the signals easily accessible to measurements by the oscilloscope. The oscilloscope (Analog Discovery Pro 3450) is then connected to a computer, which can acquire signal waveform trough the software *WaveForms*. A Teensy

[1] Nevertheless, when we did some measurements without it we did not see significant differences.

microcontroller, which is managed by the computer, is used to set the firmare on the ASIC to *test mode* and to generate a pulse which, sent to the WRD, gives origin to a test signal which is then injected into the CMBs.

A.2. Testing procedure

The testing procedure is managed by the programme `test_asics.py`, which can be found in the repository [3]. In order to test every single CMB the procedure is to fix a specific WRD and a specific D2S (both known to be properly working) and testing, one channel at the time, one CMB at the time. After this part, the same has been done to test WRDs and D2Ss, clearly fixing in the first case a CMB and a D2S, and in the second a CMB and a WRD.

The Teensy microcontroller, triggered by the computer, sends a a square pulse of $12ms$ width to the WRD. This signal is then differentiated by the WRD and sent to the D2S.

Then the computer is instructed to begin the testing process trough the command line

```
python test_asics.py -c 0 -p True
```

which runs the program, specifying in this case the channel 0 to test (`-c 0`) and starting the pulse signal (`-p True`).

A.3. Main results from the signal analysis

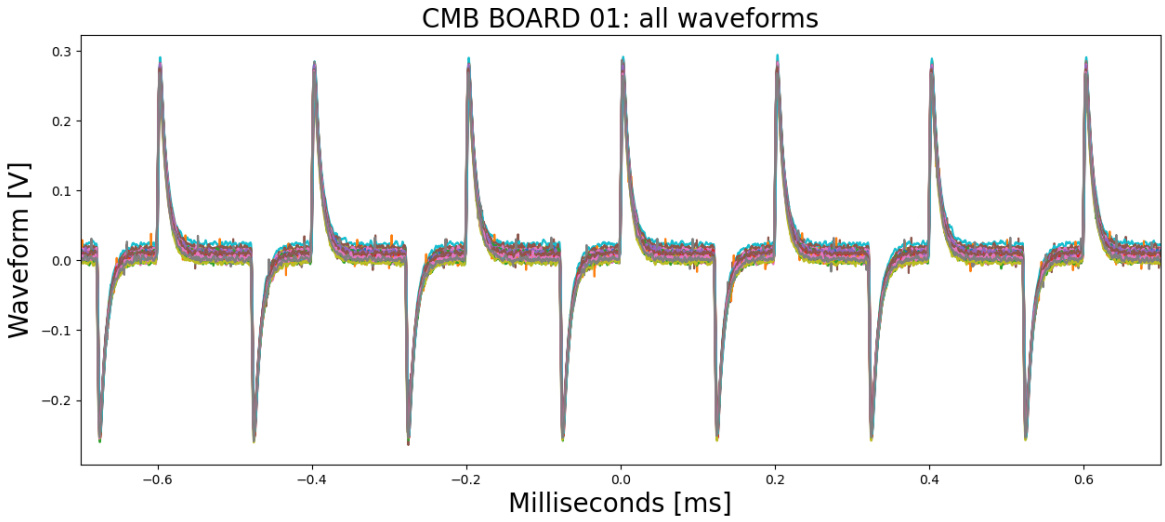

Fig. 7. The signal for all the channels. As it can be seen, all channels have approximately the same shape, pulse width and V_{pp}

.

Cold Mother Boards After repeating the procedure in the previous paragraph for every channel of the CMB that has to be tested[2], the figure 7 is obtained, after plotting all the channels on one canvas. The tests were made keeping fixed WRD-01 and D2S-01.

As it can be noticed, the amplitudes of all channels are very similar, the pulse widths[3] of the wave forms are the same and their shapes are the same too, just as expected.

After verifying the shape, a way to verify if the amplitude (thus the gain) and the pulse widths are consistent trough channels is to plot the V_{pp} and the period with respect to the channels, respectively. This yields to the graph 8.

The amplitudes and the pulse widths are mostly constant throughout channels, with some exceptions,

[2]Hence for every channel the things to change would be both the instruction in the command line and the connection to the oscilloscope so that it measures the waveform from the right channel

[3]By pulse width we mean the difference in time between the first and the second peak of the spectrum in figure 7. Since these are the derived test pulse, the time distance between peaks equals the pulse of the test signal.

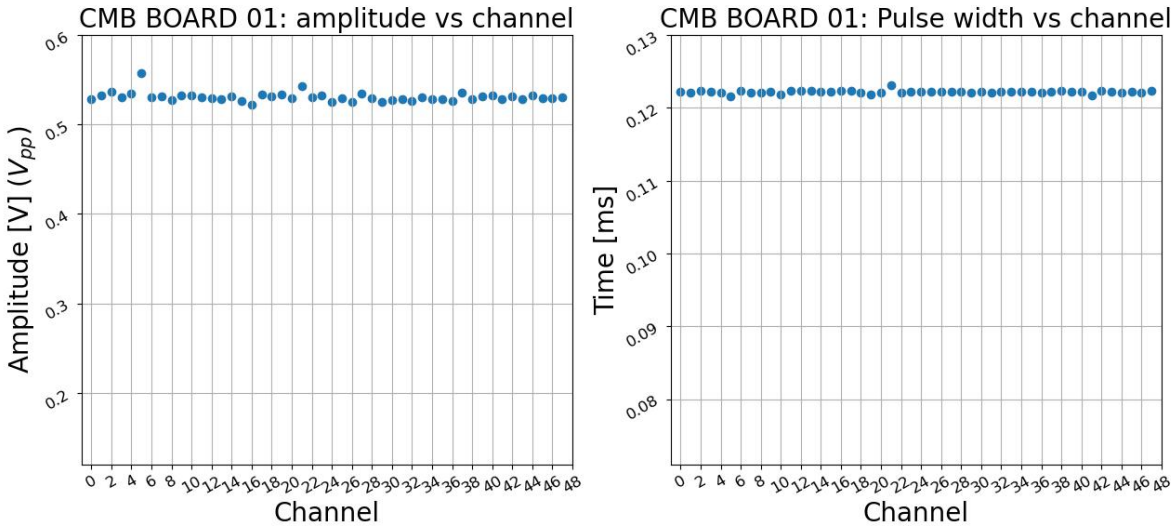

Fig. 8. All the channels and their two main parameters, with respect with the channels.

- **CMB 2**: Channels 44 and 45 have an attenuated signal (less than 50 % with respect to the other channels of the same board). Channels 46 and 47 present an almost null signal.
- **CMB 8**: channel 28 has a nearly null signal.
- **CMB 12** channel 13 has a nearly null signal.

A contains additional plots of abnormal amplitudes measured for these channels. For some CMBs there is a quite evident grouping of the channels, if we examine the amplitude vs channel graph, for example for CMB 03 (fig 9) we observe that the amplitudes of the signals, going trough the various channels, *bumps* (and stays quite consistent for a bit), for two times.

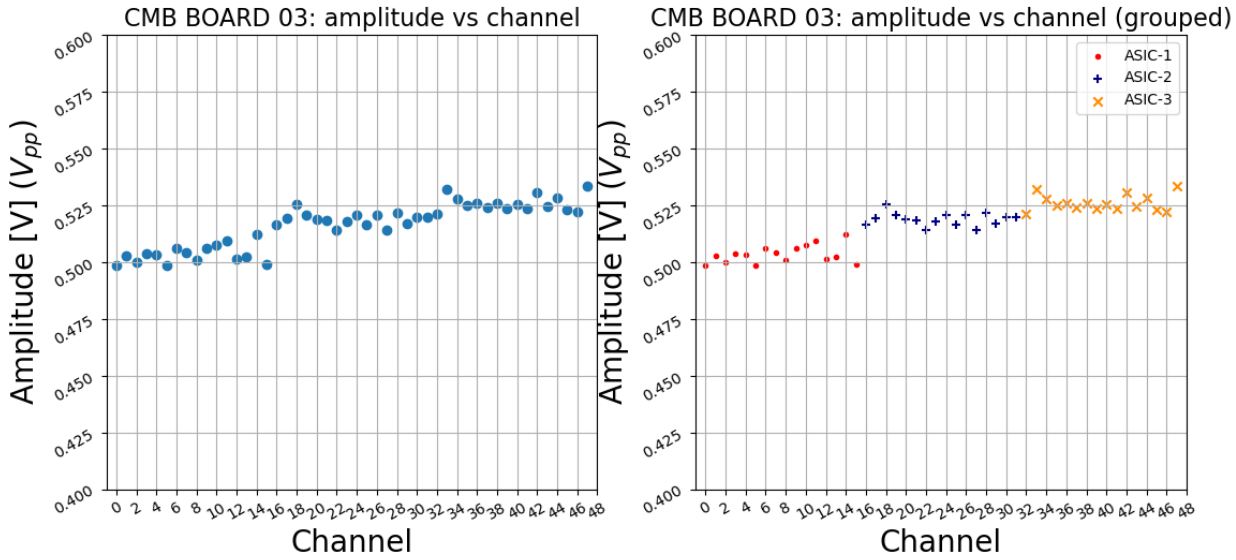

Fig. 9. The amplitude of the signals, for CMB-03 with respect to the channels.

The resulting clusters are the same we would obtain if we grouped the channels by CMB ASIC: this would suggest that the gain is ASIC dependent, maybe simply for the similar distance that the signal has to walk, coming from the same ASIC. Consequently a possible analysis is grouping by ASIC all the amplitudes of the signals, regardless of the boards they were measured. This was done in figure 10, with the carefulness of

removing the aforementioned channels which were classified as outliers. It is worth at least mentioning that we also had some troubles with the duration of some pulses: in fact for some channels we measured pulses with noticeably different periods. This problem was not systematic, since it disappeared for a second measurements. Some plots and some further comments and plots about this can be found in B.

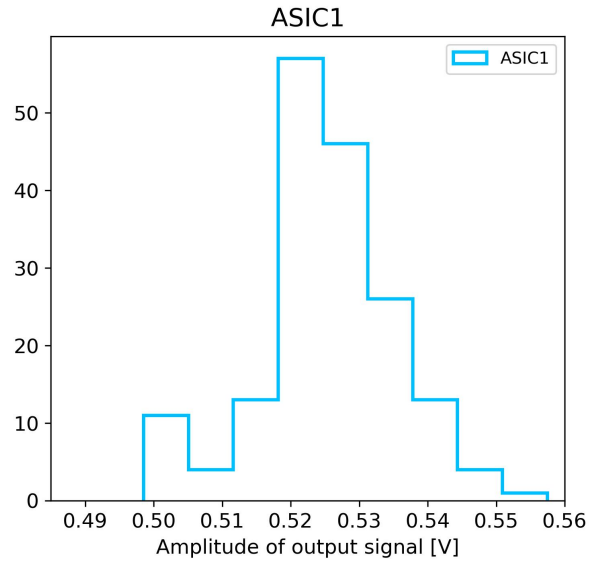

(a) The measured channels' output amplitude from all boards coming from ASIC-1

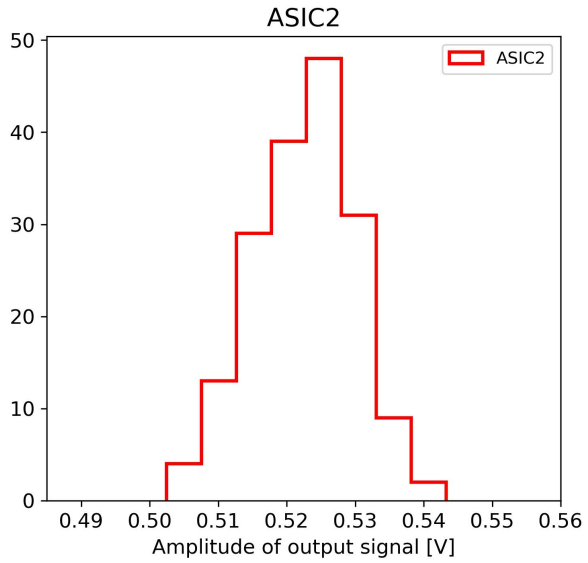

(b) The measured channels' output amplitude from all boards coming from ASIC-2

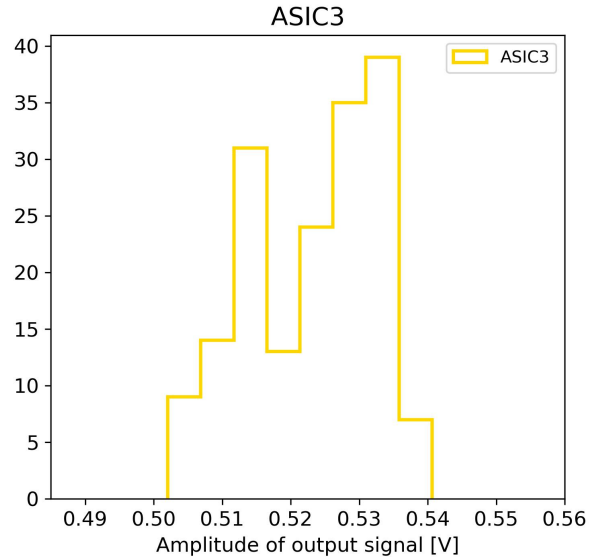

(c) The measured channels' output amplitude from all boards coming from ASIC-3

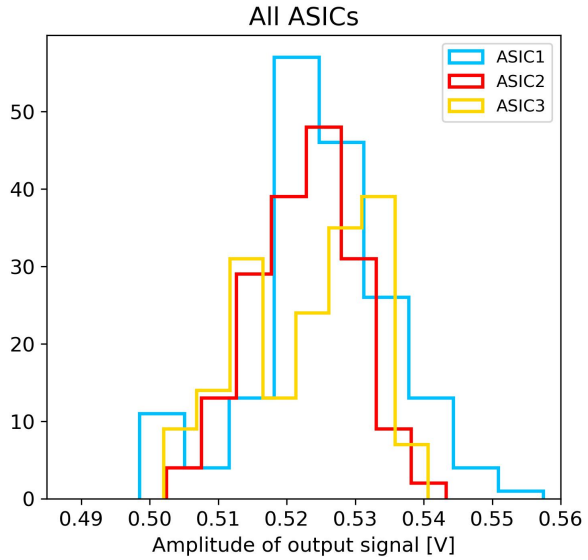

(d) The three distributions of channels' output compared

Fig. 10. The distributions of the signal's V_{pp} for all boards' channels, grouped by ASICs and then compared, for Cold Mother Boards

WRD The same procedure of the previous paragraph has been applied to test WRDs, keeping fixed CMB-03 and D2S-01. Test of WRD boards showed more prominently the ASIC dependence. We present as an example WRD02 (see figure 11a). Also in this case there was the case of a channel which had a V_{pp} less than half the average, which was the 21^{st} **of the first board**. There were some problems with periods even in this case, but as before we refer to section B.

Another remark is that figure 11b has not the form that it had in the case of 10d, but it has a second peak, for all ASICS. In all three cases the WRD for which this happens is the number 2.

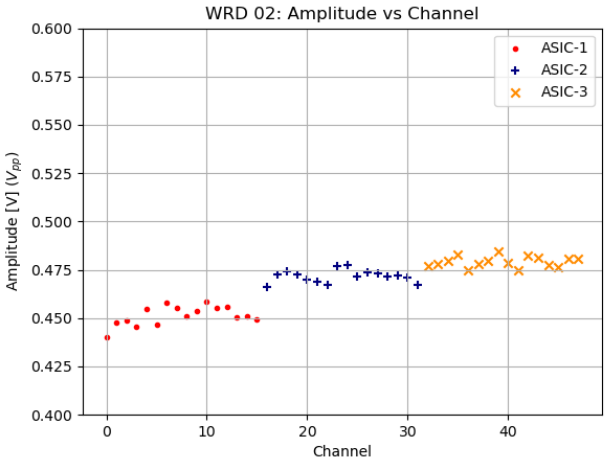

(a) Plot of V_{pp} with respect to the channel for WRD 02

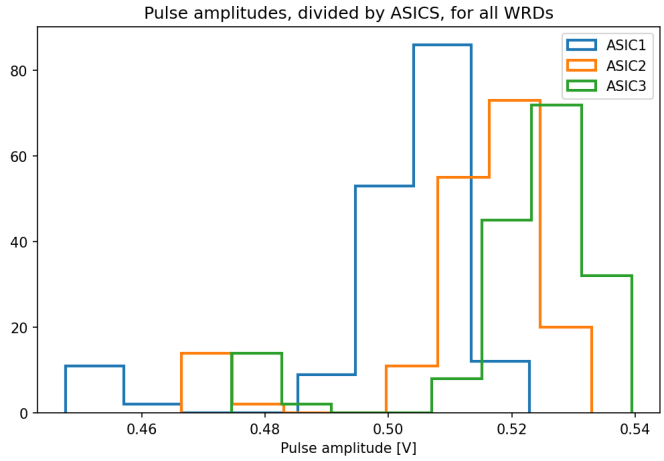

(b) The amplitudes of the pulses for **all WRDs**, grouped by ASICs.

Fig. 11. Plots for WRDs boards

D2S And lastly, we proceeded to test the D2S accordingly, keeping fixed CMB03 and WRD01. The only faulty channel was the 21^{st} **of the first D2S board**, which had a signal height of about one-tenth the average. Also in this case there channels coming from similar ASCIs were grouped, as it can be seen in figure 13b. For the jittering problems, we refer to B as before.

B. Examining the new electronic configuration

As the careful reader probably noticed, Cold Mother Boards have to be in the cryostat with the LArTPC. In order to keep argon pure and cold, the cryostat must be kept as shut as possible. This means that the wires that have to link the CMB with the outer world must pass trough some flanges; the ones that will be used during the experiment are depicted in figure 12.

As it is visible, the flanges support only DB-25 cables, but CMBs and WRDs communicate with a ribbon cable. For this reason, also two adaptors are needed to be both in the cryostat and outside of it; another adaptor must be placed outside, in order to revert the two DB-25 cables into a ribbon cable. The adaptor board used, which was costume made, is shown in 14.

After having soldered the boards, we proceeded to check the continuity of each channel, successfully, for at least two pairs of adaptor boards.

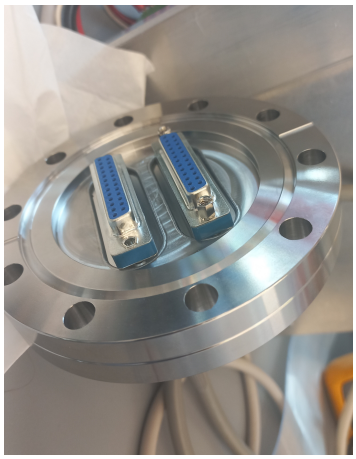

Fig. 12. The flanges that will be used during the experiment

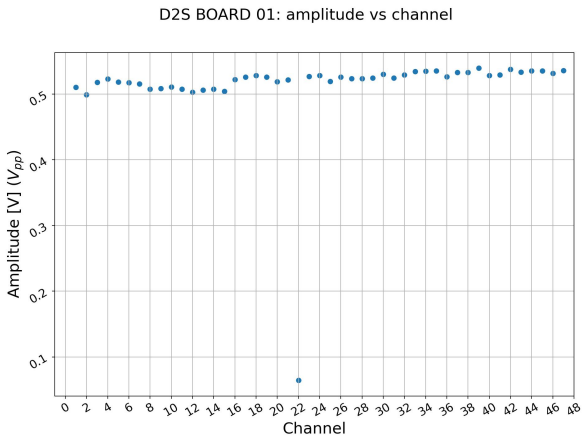

(a) Plot of V_{pp} with respect to the channel for D2S 01

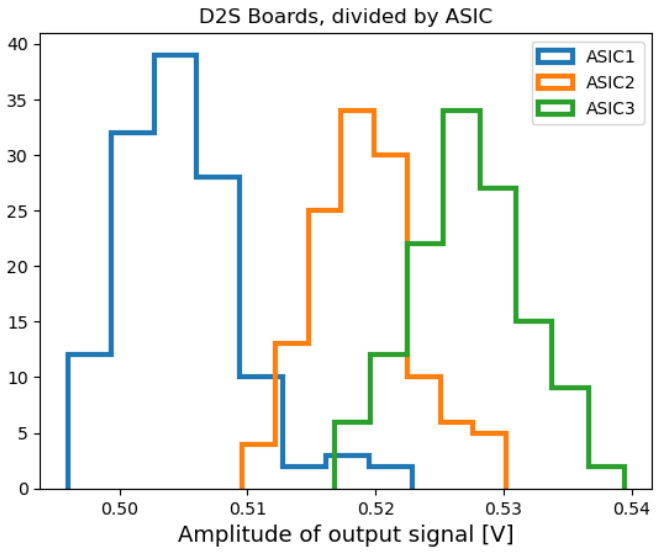

(b) D2S boards divided by ASIC.

Fig. 13. Plots for D2Ss boards.

B.1. Cold test

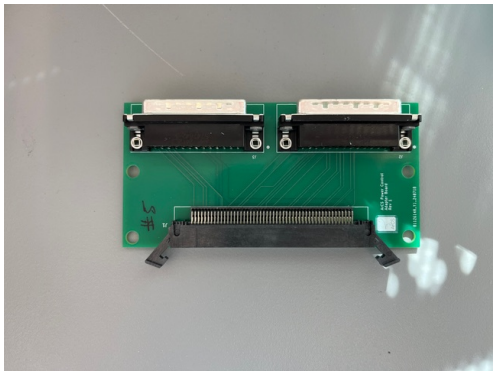

Fig. 14. Adaptor board from DB-25 cables to ribbon cables

While Cold Mother Boards and the ribbon cables have already withstood cold temperatures, the DB-25 cables and the adaptor boards have not been stressed to those conditions yet. Therefore it is necessary to do a *cold test*. To do so we accessed the cryogenic testing facilities. For the test, we used a dewar filled with liquid Nitrogen, which has a boiling point lower than liquid Argon, hence it's an even stronger stress test than the one it should be able to bear. We left the boards with a pair of DB-25 cables in the bin for 30 minutes. Eventually, we tested the continuity of the expected channels, finding that it was verified for the expected channels.

3. SOFTWARE DUTIES

A. The simulation

A.1. G4beamline

G4beamline is a software tool based on Geant4, designed for simulating the passage of particles through matter and their trajectories in beamlines of particle accelerators ([7]). Used in particle physics and high-energy experiments, G4beamline allows users to model and visualise complex geometries, electromagnetic fields, and particle interactions with detectors and materials. A key feature of G4beamline is its ability to describe even complex experimental setups through an intuitive, simple scripting system, without the need for users to write C++ code, while providing a practical graphical interface. With configurable commands, users can define beam configurations, geometry, and magnetic fields, obtaining detailed simulations that provide accurate results for studying beamlines and experimental apparatuses. We are going to use this software to simulate the beamline of the experiment.

A.2. The simulation and its goal

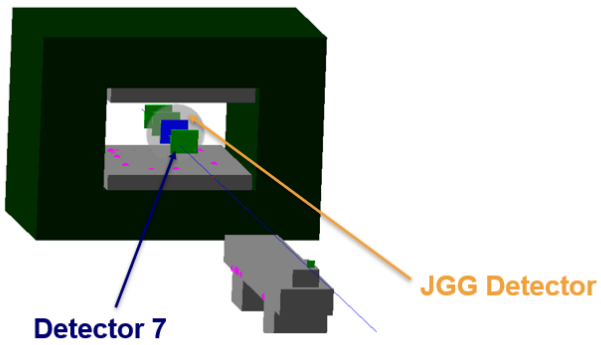

Fig. 15. The virtual detectors in the G4beamline simulation.

The simulated apparatus is depicted in figure 4 (which is a result of G4beamline's graphic display), considering a 64 GeV gaussian beam of π^+, with a $\sigma_x = \sigma_y = 2mm$.

The goal of the simulation is to understand how the distributions of electrons passing trough two virtual detectors (one placed immediately before and one inside the the JGG) vary with respect to the module of the magnetic field. The detectors are called Detector7 and JGG Detector, respectively, and they are so-called *virtual detectors*; figure 15 depicts their position.

This means that they have a 100 % efficiency and essentially measure the particles passing trough their volume without disturbing them in any way. In other words, they are purely ideal detectors, which make us understand the composition of the beamline at a certain point in space, with no error in measurements and without introducing any bias. All the simulations scripts can be found in [3].

The simulations run had for each one a different scaling of the magnetic field. The JGG manget can supply a maximum field of 0.7T, but ideally we would like to use the minimum field possible, that allows

- ! Charge separation, better momentum measurements and distinction of electronic and photonic showers (which don't happen if the field is too low).
- ! To have a sufficient rate for both the detectors and having a spectrum that stays mostly unaltered.[4]

Decreasing the magnetic field is beneficial both for technical and economical reasons; the goal of this specific simulation is understanding how lower magnetic fields impact on the electron's spectrum before and after the JGG. The other point shall be the object of other future simulations. For all the simulations around 150 milion events were simulated, except for the ones with field equal 0.49T and 0.7T, for which the number of events was doubled.

B. Analysis

The first step was simulating the beamline, considering a field of 0.7T and then halving it. The first possible thing to see is the counts of the two detectors, in this two cases, considering only the particles going trough both detectors (coincidences).

[4] For this point, we have to be careful that the simulations for the field with module $0.7T$ and the one with module $0.07T$ have double the events.

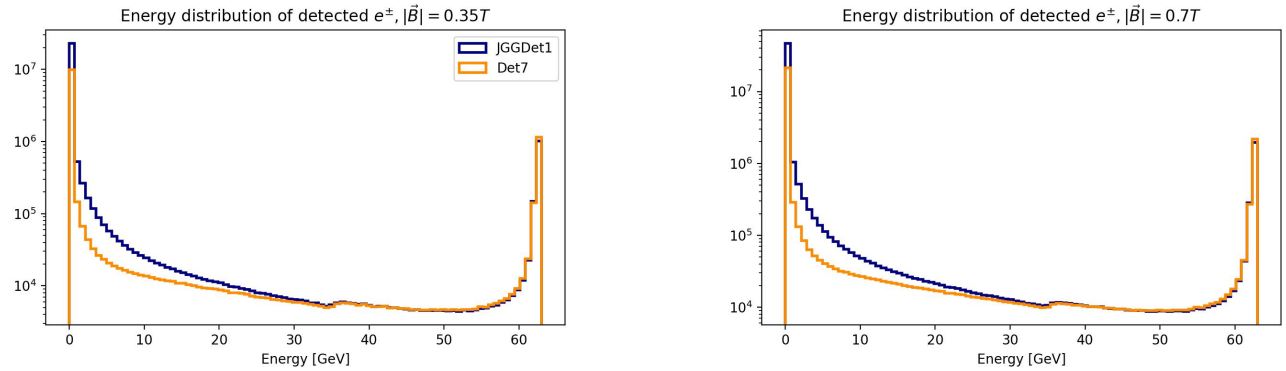

Fig. 16. The spectrum of the configuration with the field $|\vec{B}| = 0.35T$ and $|\vec{B}| = 0.7T$

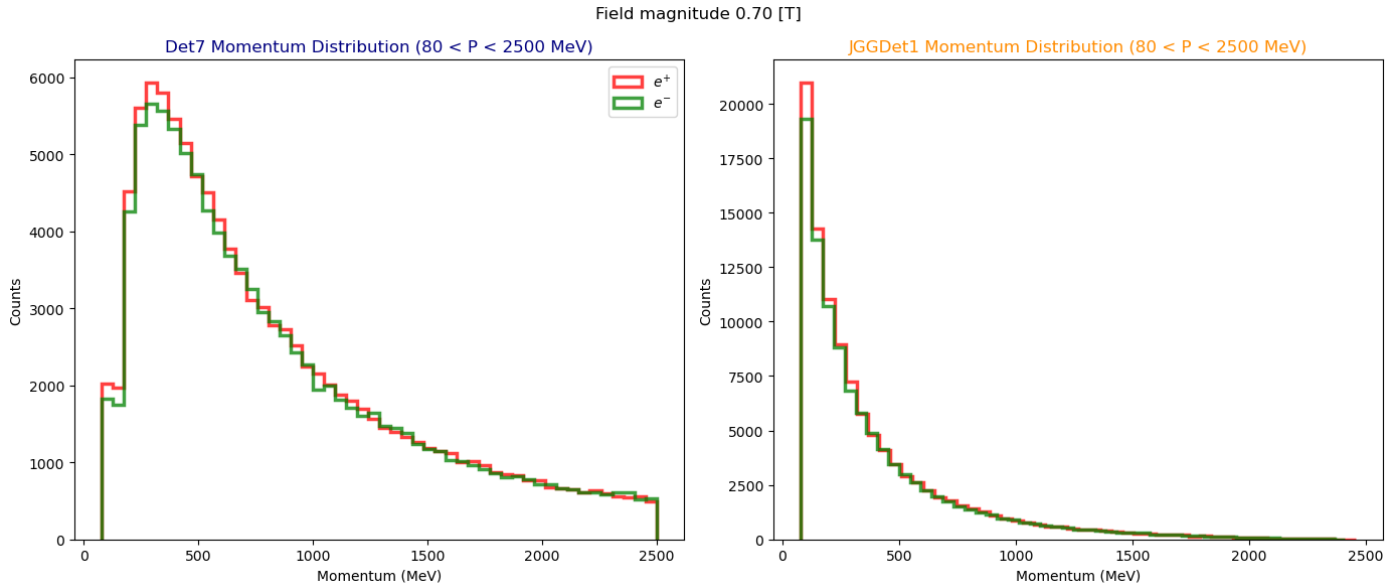

Fig. 17. The spectrum of electrons and positrons, considering the energy range from 80 to 2500 MeV, for a 0.7T field in the JGG.

As it is possible to see from the figures 16 the electrons and positrons from the second detectors are in general less energetic than the first ones, as a consequence of the interaction with the detecting medium. Nonetheless, we are not interested to the whole energy spectrum, since the electron's energy that are produced by events of interest are in the energy range from 80 to 2500 MeV. In figure 17 it is possible to see the spectrum in the range is very similar for both detectors, both in shape and in average value: in fact for electrons in the Det7 detector is $\langle|\vec{p}|\rangle = 484.2 \pm 0.9 MeV$ and for the JGG detector it is $\langle|\vec{p}|\rangle = 413.8 \pm 0.5 MeV$.

The immediately consequent question is what is the resulting spectrum in the case of an halved spectrum. It is possible to see in figure 18 that the shape and also the average of the spectra remain almost unaltered (the mean is fact, $\langle|\vec{p}|\rangle = 515.6 \pm 1.4 MeV$ for the Det7 detector and $\langle|\vec{p}|\rangle = 430.2 \pm 0.7 MeV$ for the JGG detector). As an extreme case, we show in figure 19 shows practically the same spectrum for a field one tenth of the maximum. Even in this case, both the shape and the average value of the momentum were not largely effected by the variation of the field.

We therefore present the average of the electron's momentum with respect to the magnetic field modulus in fig 20; the values are also in table 1. As it can be seen, it is not very affected, even for a wide span fields values. It was also worth noticing that the number of coincidences does not change significantly a lot with varying the magnetic field: in the case of the maximum field the events in 17 are more just because for that maximum field case the number of events simulated was double with respect to the others. Equivalent results for this trend are found for positrons.

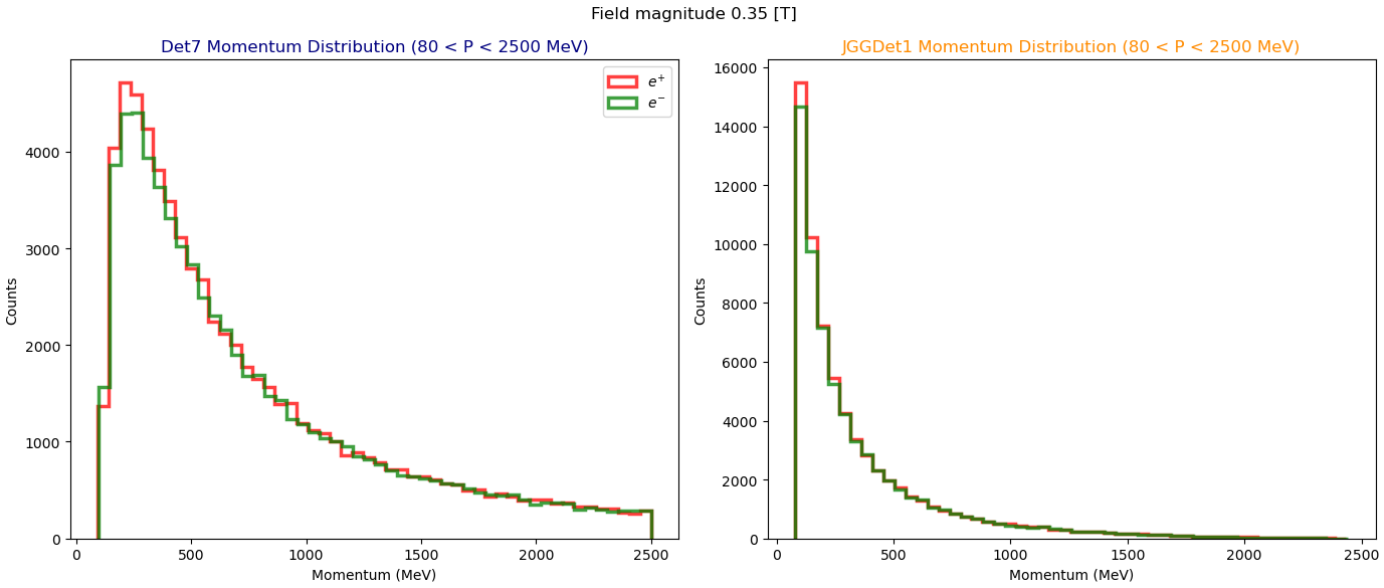

Fig. 18. The spectrum of electrons and positrons, considering the energy range from 80 to 2500 MeV, for a 0.35T field in the JGG.

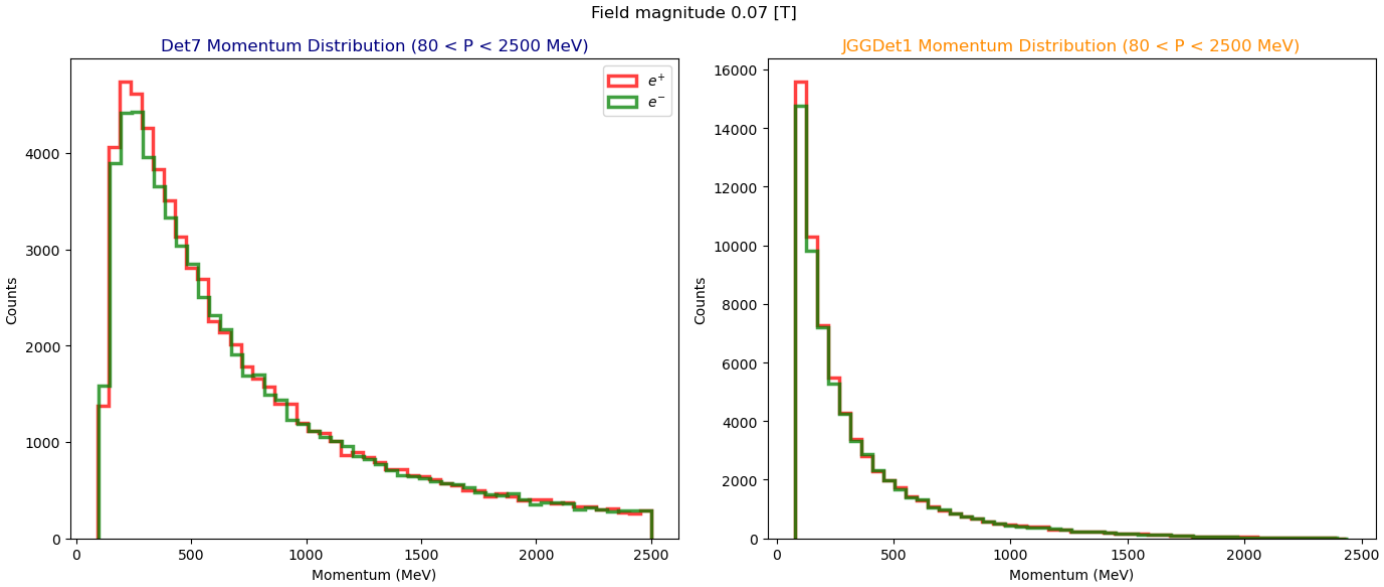

Fig. 19. The spectrum of electrons and positrons, considering the energy range from 80 to 2500 MeV, for a 0.07T field in the JGG.

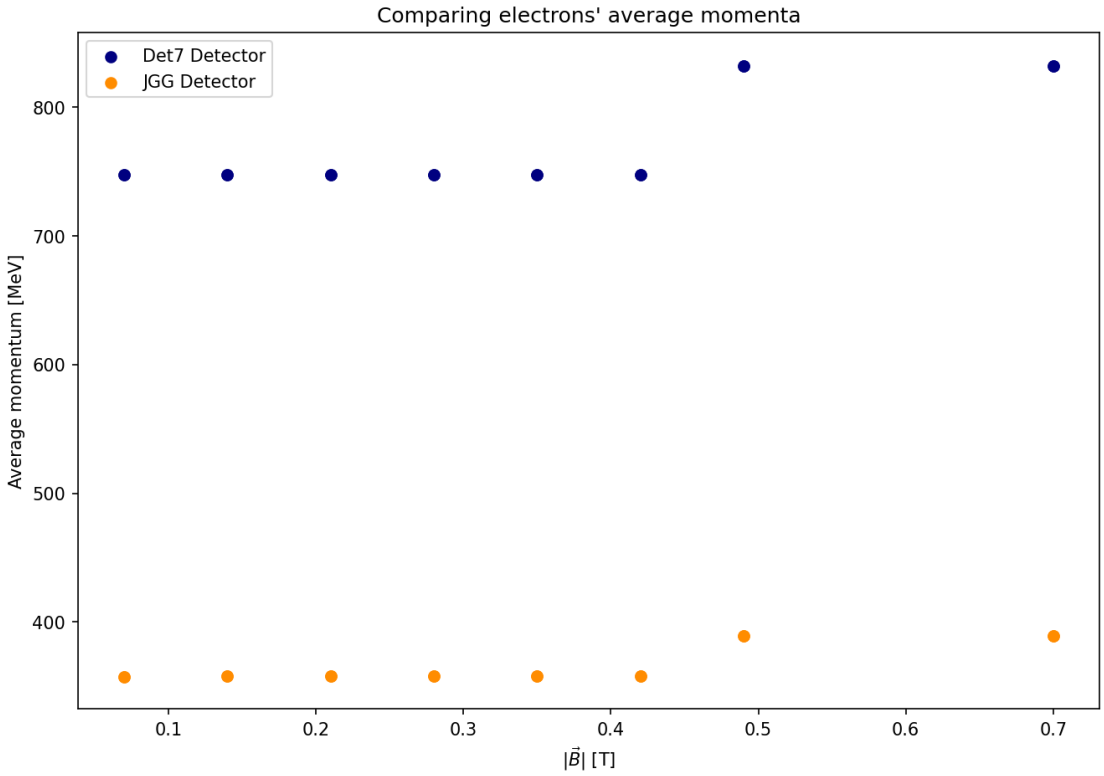

Fig. 20. The average momentum of the electrons, varying the magnetic field.

$\lvert\vec{B}\rvert[T]$	$\langle\lvert\vec{p}\rvert\rangle[MeV]$ (Det7)	$\langle\lvert\vec{p}\rvert\rangle[MeV]$ (Jgg)
0.07	747.41 ± 2.87	357.73 ± 1.31
0.14	747.51 ± 2.87	357.78 ± 1.31
0.21	747.52 ± 2.87	357.76 ± 1.31
0.28	747.44 ± 2.87	357.76 ± 1.31
0.35	747.57 ± 2.88	357.86 ± 1.31
0.42	747.53 ± 2.87	357.79 ± 1.31
0.49	831.50 ± 2.55	389.04 ± 1.09
0.7	831.50 ± 2.55	389.04 ± 1.09

Table 1. Average momentum for different values of the magnetic field, considering particles only in the range from 80 MeV to 2500 MeV, for both detectors. The error is computed as $\frac{\sigma}{\sqrt{n}}$, where σ is the sampling variance and n is the number of events.

4. CONCLUSIONS

The work done here can be summarised in the following bullet points

- Among the CMBs that were tested most of them were working properly; the only ones that gave problems were number 2, 8 and 12.
- For WRDs the only problematic board was number 1, specifically the 21^{st} channel.
- For D2Ss the only problematic board was number 1, specifically the 21^{st} channel.
- The test for the continuity of the adaptor boards and the cables connecting them gave positive results
- The simulation revealed that decreasing the magnetic field does not affect significantly the momentum of the detected electrons, nor the shape of their spectrum.
- Even though the number of electrons is changed by varying the magnetic field, the number of coincidences is still high enough for our purposes.

5. ACKNOWLEDGEMENTS

First of all, I would like to thank my supervisor Marco Del Tutto: I was honoured to collaborate with him. Not only he has been of great help throughout my internship, but he was also a wonderful person to work with. I also praise all the other people in the ArCS collaborations, who gave me valuable insights and suggestions during my internship, creating a collaborative and stimulating environment. I sincerely express my gratitude to the organising committee of the Italian summer school program at Fermilab, which has granted me this wonderful opportunity, especially prof. Simone Donati and Dr. Marco Mambelli. I would like to show also my appreciation for all the other students who were part of the internship too, and went along me trough many of the challenges and the adventures I faced, in particular my roommates who most of the times made me feel home during the evenings and the nights, and the neutrino division people, who bore me during the working hours (and not only). I furthermore thank Tanya, the bartender from the User's centre, that with her kindness and her smile filled my post-work evenings. Finally, I thank the US and the great state of Illinois, for providing me happy memories that I will happily keep for as long as I can, as long as one of the best live concert by *Lawrence the band*.

A. EXAMPLES OF NON EXPECTED CHANNEL BEHAVIOURS

A. Amplitude

Here we present some of the possible problems presented by non functioning boards. As previously said, one of the most problematic was CMB 02, as it is possible to see in 23. We also present the signal amplitudes with respect to the other channels, for all the boards that have at least one channel whose V_{pp} is significantly lower than the others.

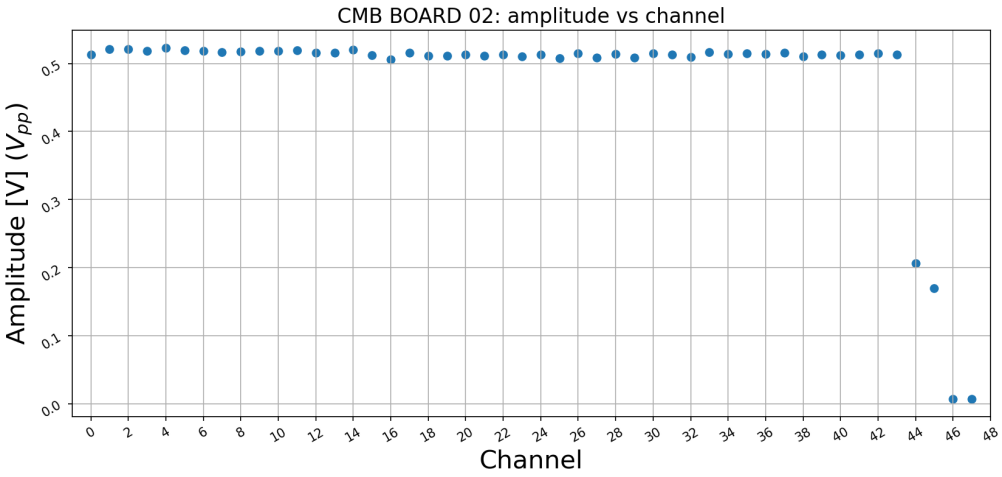

Fig. 21. CMB 02 amplitude of signals, with respect to the channels.

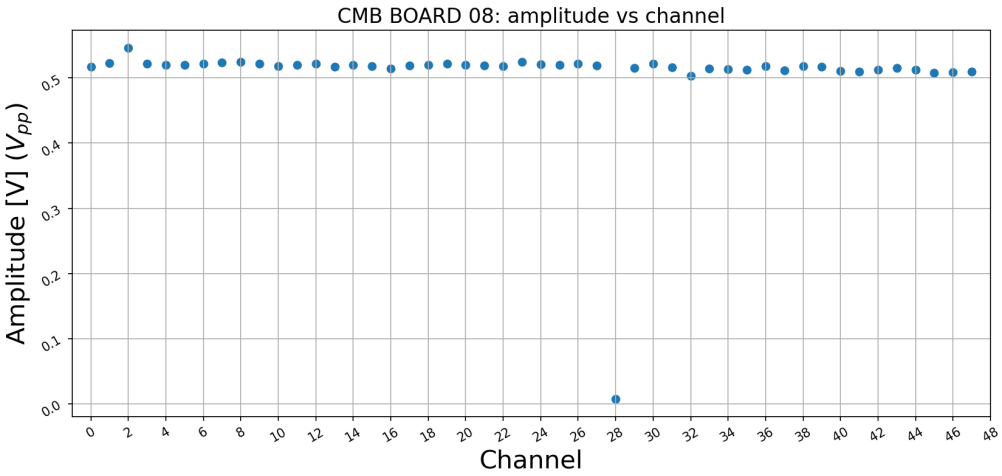

Fig. 22. CMB 02 amplitude of signals, with respect to the channels.

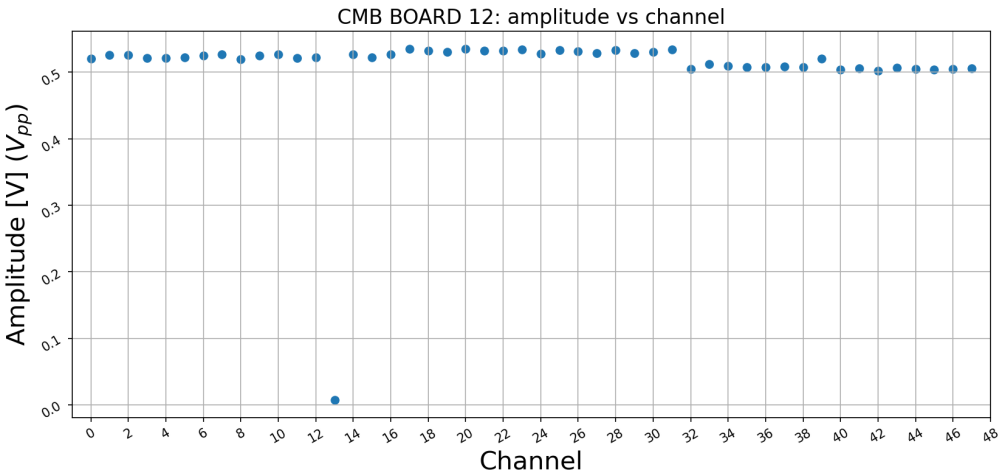

Fig. 23. CMB 08 amplitude of signals, with respect to the channels.

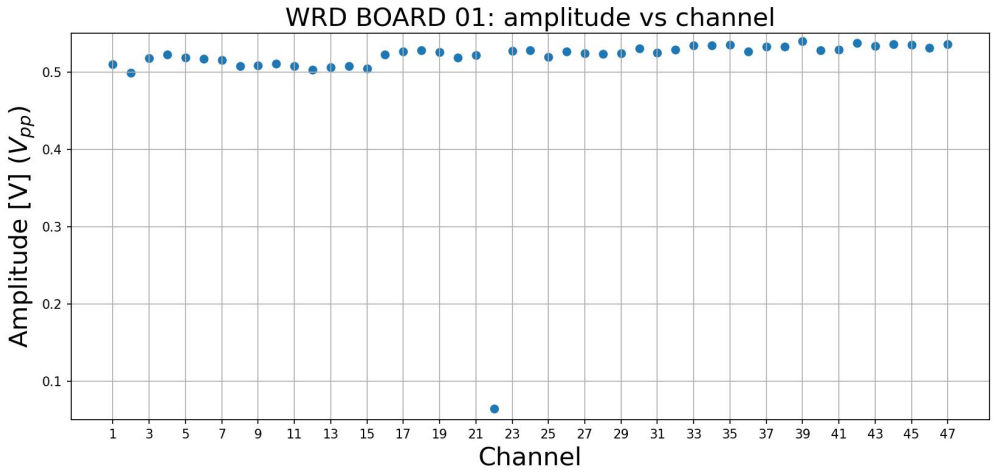

Fig. 24. WRD 01 amplitude of signals, with respect to the channels.

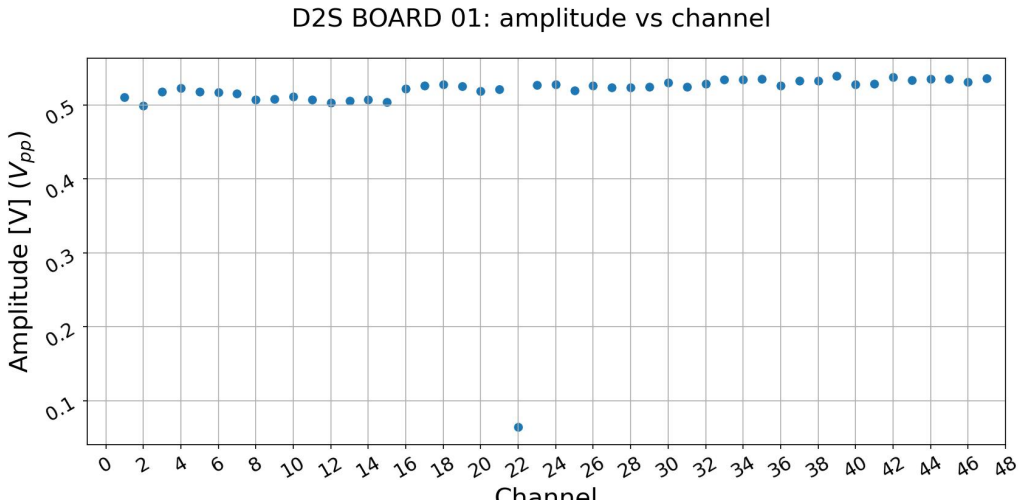

Fig. 25. D2S 01 amplitude of signals, with respect to the channels.

B. Time period

Let's consider the plot of the resulting signals from each channel of CMB01, in figure 7. At first glance, the time difference between a positive peak and the following negative is both constant throughout the measurement and constant trough channel. If we plot the time difference versus channel looks like figure 26. As it can be seen, there is no evident dependence of the period with respect with the channel.

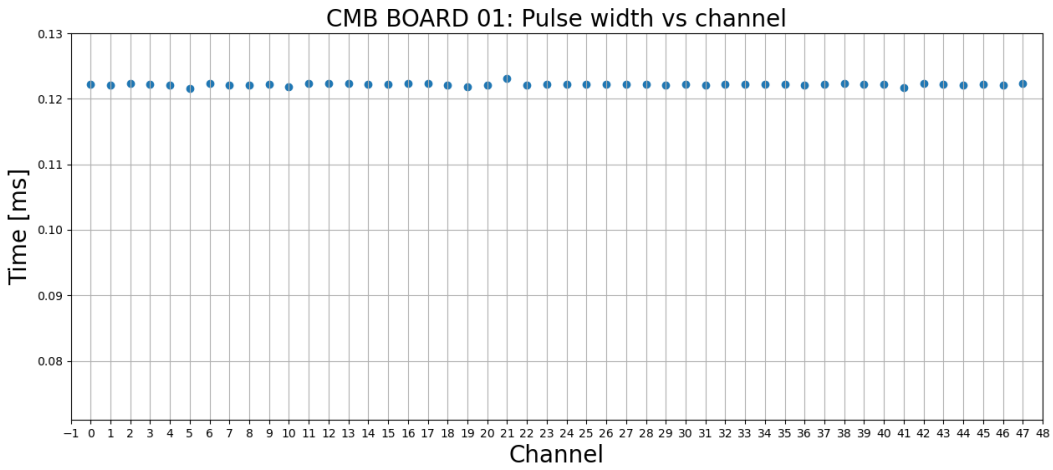

Fig. 26. Pulse widths for CMB01, by channel.

It is anyway as we expect it: the testing signal is always the same (a 12 ms square pulse) which is injected in the WRD. This board derives it and feed it to the CMBs; after that there is the signal goes trough the WRD again, and then the D2S, to be eventually read out by the oscilloscope. Nevertheless during the tests, some difficulties were encountered because, for some boards, it appeared that the period was not the same for all channel: for the measured signals were as shown in 27.

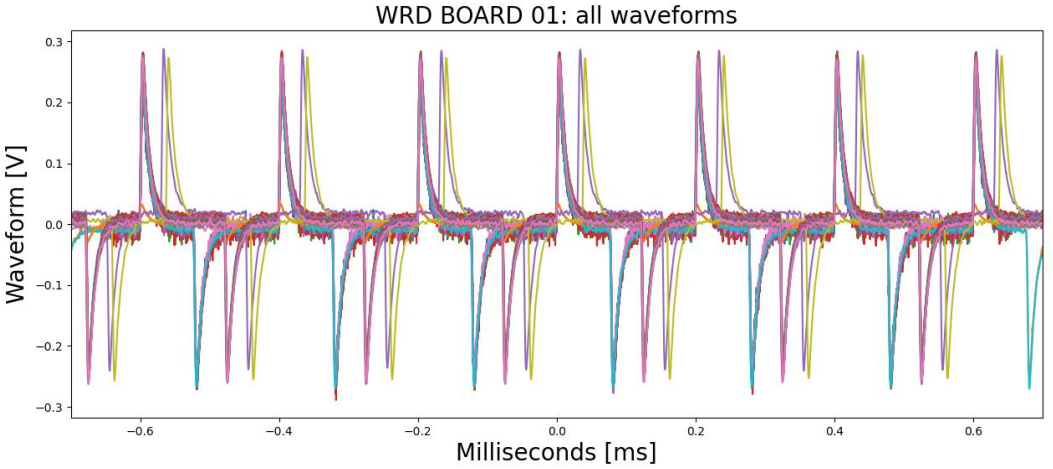

Fig. 27. The first measurement of the outputs of WRD01 showed clear signs of jittering

This was quite peculiar: a change in gain is reasonable to be variable for different channels, while the period should not be affected, since the input signal is always the same. Plotting hence the time difference with respect to the channel, we can see that, in this case channels could be divided in ones that had a pulse width of $\approx 12ms$ and others that had a pulse widths of $\approx 8ms$ (see 28). Upon a second measurement, this problems disappeared, and that is why this discussion has been relegated to a mere appendix.

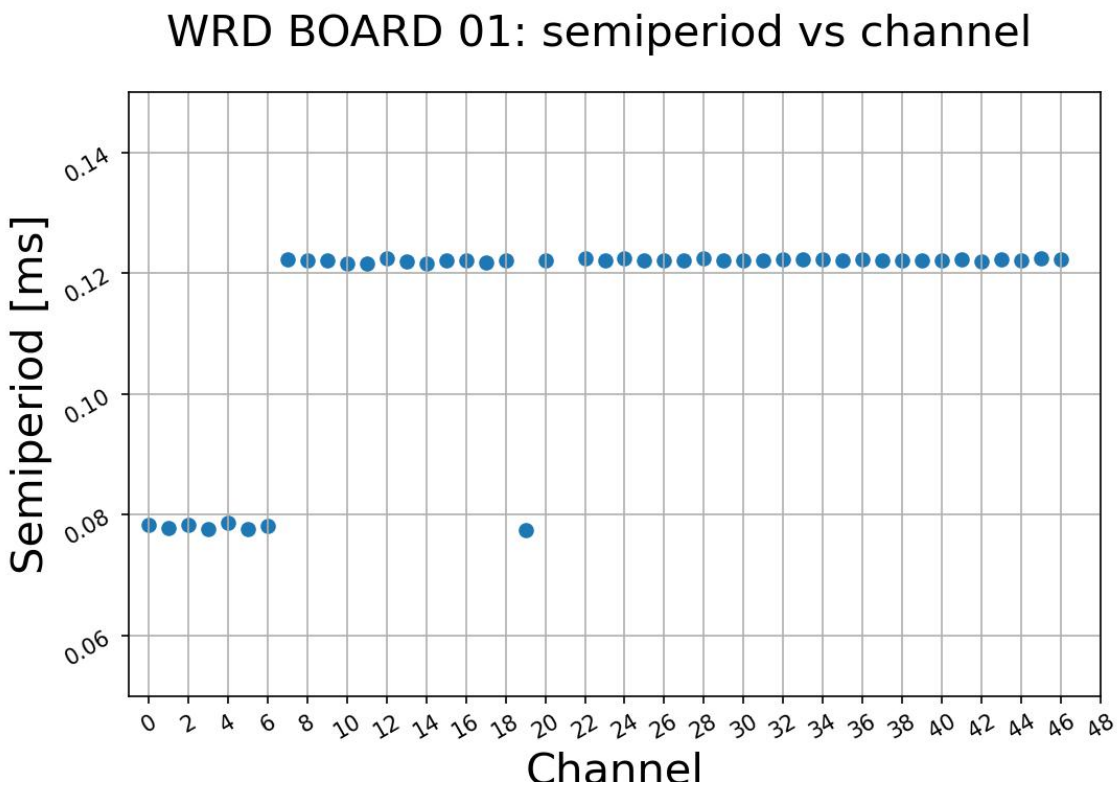

Fig. 28. The pulse widths of WRD01 are not the same for all channels

Usually, most of the boards that presented this kind of problem, did it for only one channel. We briefly list all the boards that presented this problem:

- **CMB**: board number 1, 6 and 8
- **WRD**: board number 1 and 5
- **D2S**: board number 1 nad 7

We believe that the problem was caused by the clock given by the computer to the microcontroller, which we suppose it was not always the same.

LIST OF FIGURES

REFERENCES

[1] R. Acciarri et al. "The Liquid Argon In A Testbeam (LArIAT) experiment". In: *J. Instrum.* 15.04 (Apr. 2020), P04026–P04026. ISSN: 1748-0221. DOI: 10.1088/1748-0221/15/04/p04026. URL: http://dx.doi.org/10.1088/1748-0221/15/04/P04026.

[2] Marco Del Tutto et al. *A Liquid Argon Time Projection Chamber in a Magnetic Field*. Fermilab LDRD Proposal. Lead Division: Neutrino Division. 2024.

[3] ArCS Collaboration. *ArCS github repository*. URL: https://github.com/ArCS-FNAL.

[4] Richard Clinton Fernow. *Introduction to experimental particle physics*. Cambridge University Press, 2022.

[5] Dean Shooltz. *LArIAT TPC Front-end electronics Documentation package version 1*. Sept. 2015.

[6] M. Tanabashi et al. "Review of Particle Physics". In: *Phys. Rev. D* 98 (3 Aug. 2018), p. 030001. DOI: 10.1103/PhysRevD.98.030001. URL: https://link.aps.org/doi/10.1103/PhysRevD.98.030001.

[7] Tom Roberts. *G4beamline User's Guide*. Accessed: 2024-10-09. Muons, Inc. 2024. URL: http://www.muonsinternal.com/muons3/G4beamline.